Deblending of simultaneous and flip-flop shooting of sparse node long offset seismic for refraction FWI

Himadri S. Pal, Hassan Masoomzadeh, Henrik Roende, Zhaojun Liu, Duncan Bate and Chuck Mason, TGS*

Summary

We present the modeling of blended acquisition for a node survey acquiring long offsets (50 km) with a focus on the low-frequency diving waves. The synthetic data simulates six sources, with shots fired both simultaneously and in flip-flop formation. The diving waves are recovered using an iterative inversion-based deblending methodology, which would subsequently be used for refraction FWI. Acquisition options are studied using different shot firing orders, source vessel spacing, dither time, and background noise. We show that this deblending methodology successfully recovers useful signal across a wide range of acquisition geometries and firing patterns. The success of deblending in recovering the diving waves is quantitatively established.

Introduction

Full waveform imaging (FWI) can provide significant uplift in velocity-model fidelity, thus reducing uncertainties in seismic imaging. For complex Gulf of Mexico geology, appropriately sampled data, very long offsets, and recording of low frequencies are all critical for deeper FWI model updates [Mao et al., (2016), Shen et al., (2018), Tiwari et al., (2019)]. Due to the ubiquitous presence of complex salt in this region, very large offsets and long travel time recording is required to detect diving waves critical for refraction FWI.

An ocean bottom node (OBN) survey can record critical full azimuth seismic with relatively low background noise. The economics dictate a sparse-node layout but recording a full azimuth grid of seismic is feasible with a dense carpet of shots. Blended shot recording is necessary to acquire such densely shot data over a large area, in order to shoot all shots and avoid rolling the nodes. This study investigates the feasibility of extracting the very weak long-offset (up to 50 km) diving waves from overlaying strong primary signal from other guns and source vessels. We also investigate the acquisition parameters best suited for deblending diving waves for FWI, before the seismic is acquired. The subsequent sections describe the synthetic receiver gathers used as the true target, and the blending schematics based on different acquisition geometry and parameters. Simultaneous shot and flip-flop shot sequences are analyzed and compared. The deblending results are analyzed for different acquisition uncertainties and background noise.

Sparse node OBN blended synthetic

The acquisition geometry is shown in Figure 1. The nodes will be laid out with 1 km inline and 1 km crossline separation, due to tether length on umbilicals for ROV deployment. Three source vessels with two guns each will navigate the source grid in a racetrack pattern. The crossline separation between the adjacent source vessels is 2 km. Two different source configurations are considered for this study. One consists of both sources on the same vessel firing simultaneously (SS), separated only by a small random dither time. The second scenario is where the two guns on a source vessel fire in a flip-flop (FF) fashion every 25 m, with a random dither time added. Subsequent firing of the same gun occurs 50 m apart in both scenarios with a 100 m source separation.

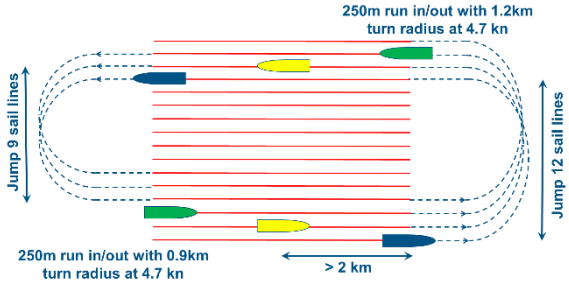

Figure 1: Racetrack shooting schematic for node acquisition with 3 vessels maintaining 2 km source vessel separation. Not drawn to scale. (courtesy Magseis Fairfield)

A single receiver gather synthesized by acoustic modeling is used to generate the single gun synthetic data. The maximum offset is 50 km, with 50 m shot inline spacing, and 100 m crossline spacing, and the record length is 40 s. The frequency range of the synthetic is from 2 Hz to 8 Hz, which is adequate for refraction FWI. Figure 2a shows the target synthetic with added random noise. The background noise pattern is pseudo-random, uncorrelated to the signal and simulates background noise during acquisition. The very weak diving waves arriving the earliest are no longer distinguishable. It is evident that the noise dominates these weak diving waves, and since this random noise cannot be predicted, recovering the diving waves gets especially difficult. Several shot lines are used to generate the blended synthetic seismic data. To generate the multi-shot blended data, the individual traces are shifted and overlaid according to the shot firing times, which include shot-to-shot delay as well as a random dither. The blended SS data created with a Gaussian random dither time with 500 ms standard deviation is shown in Figure 2b. In this example shot line, one of the guns produces a coherent signal, while the other fires at

10.1190/segam2019-3216467.1

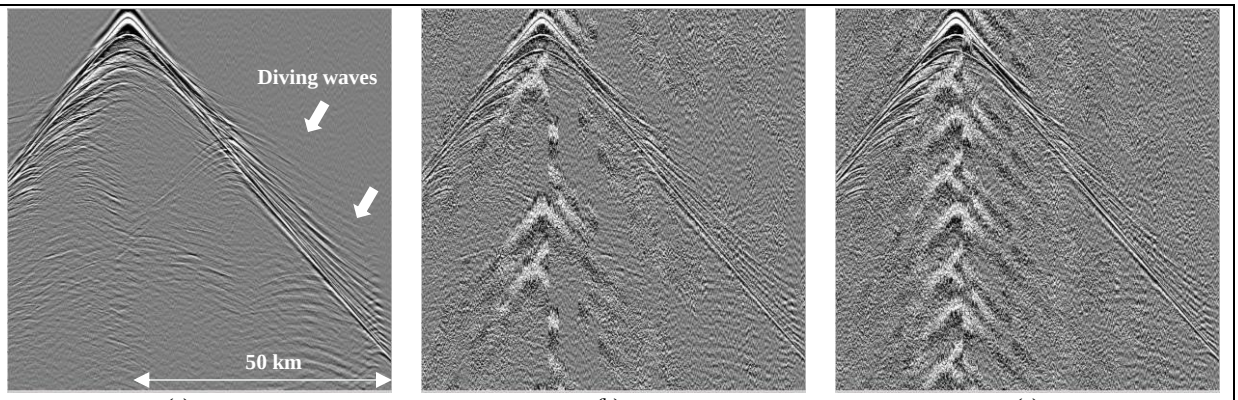

Figure 2: Synthetic receiver gather for a shot line (a) target with background random noise added, (b) blended with SS configuration, and (c) blended with FF configuration.

similar times with a random dither. This causes the signal from the second gun to appear as a random noise overlaying the primary events. Similar blended data in FF shot configuration is shown in Figure 2c. An advantage of SS over FF shot is less self-blending, as the guns from the same source fires 50 m apart instead of 25 m, potentially yielding a longer stretch of clean signal.

Deblending Methodology

Several deblending methodologies exist for separating the primary source signal from a blended acquisition. One such method of extracting primary source using sparse inversion has been proposed by Abma et al. (2010). Another enhanced adaptive subtraction (EAS) method proposed by Liu et al. (2014) uses iterative denoise and adaptive subtraction. The random noise is iteratively estimated for each of the different sources to gradually improve the noise model. Masoomzadeh et al. (2017) presented an inversion-based method of iteratively thresholding and isolating strong coherent events in 3D f-k_x-k_y domain. Deblending methodologies must be chosen and optimized carefully based on acquisition type and data quality. In this case, the very weak diving waves at the far offsets need to be recovered from the much stronger noise from blended sources, as well as other random noise. We applied the 3D f-k_x-k_y domain inversion-based deblending for both SS and FF acquisition, using the same processing parameters for both cases.

Results

The above-mentioned deblending methodology is applied to the blended data, and the diving waves are analyzed. A 3D view of blended and deblended data overlay is presented in Figure 3, showcasing how well the extreme long offset diving waves are extracted. Deblending is most accurate when random noise is not present, as shown in Figure 4. Figures 4a and 4b show the deblended data for the SS and FF acquisition respectively. These results demonstrate that it is possible to distinguish all the diving wave signals, even at extremely far offsets. There is little amplitude drop in the deblending results due to leakage for the earliest arriving signal, and at extremely far offsets. The percentage amplitude decay compared to the target for the SS acquisition case is quantified in Figure 4c. The relatively strong diving waves are recovered efficiently, with almost no drop in amplitude. The weak refractions have less than 10% loss in amplitude. The amplitude loss for FF acquisition is quite similar. Figure 4d shows the difference between the SS and FF amplitude levels, as a percentage of the target. It is interesting to note that there is no significant change in the deblending result with the change in shot configuration, any

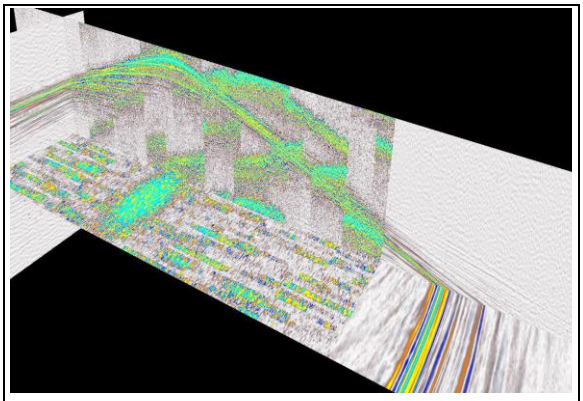

Figure 3: 3D view of blended and deblended seismic

10.1190/segam2019-3216467.1

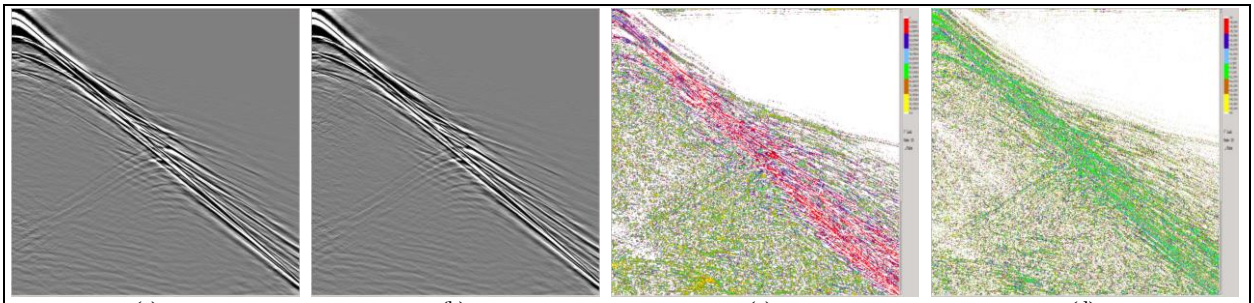

(a) (b) (c) (d)

Figure 4: Synthetic receiver gather for a shot line without added noise for (a) deblended with SS configuration, and (b) deblended with FF configuration, (c) percentage amplitude drop for SS (red denotes less than 15% drop, about 1~2 dB drop), (d) amplitude drop for FF compared to SS (green is less than 15% difference).

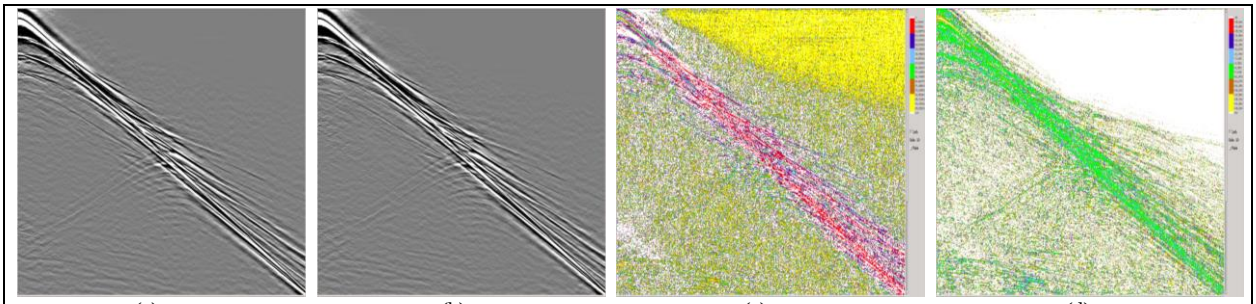

(a) (b) (c) (d)

Figure 5: Synthetic receiver gather for a shot line with added background noise for (a) deblended with SS configuration, and (b) deblended with FF configuration, (c) percentage amplitude drop for SS (red denotes less than 15% drop, about 1~2 dB drop) , (d) noise-free deblending minus deblending with noise for SS (green is less than 15% difference).

difference is mostly random. This is because the level of noise contamination from other guns depends mostly on the total number of sources, rather than the relative firing sequence of those sources.

In the presence of background random noise, the deblending performance degrades as expected. Figures 5a and 5b show the deblended receiver gathers for input shots of Figures 2b and 2c respectively. Comparing to the target shot gather (Figure 2a), all the diffractions are distinguishable. There is little difference between the SS and FF shot patterns, just like the background noise free versions before. The relative drop in amplitude of the SS deblended gather over the target is expressed as a percentage in Figure 5c. Even in the presence of noise, the strong refractions and diving waves are easily recoverable, recognized in red in that figure, with only a 10 - 15 % drop in amplitude. This corresponds to a less than 2 dB loss in signal due to deblending. Our conclusions are very similar for the FF shot data. The difference in deblending due to the background random noise is quantified in Figure 5d, which is the absolute amplitude difference of the noise free deblending and the one with noise, expressed as a percentage of target amplitude. Most of the refractions have less than 15% amplitude loss, although this depends on severity of the noise.

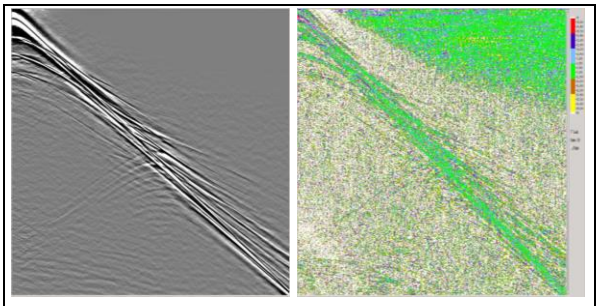

(a) (b)

Figure 6: SS data with 1000 ms dither (a) deblended gather, and (b) difference from 500 ms data as percentage of target (green is less than 15% difference).

10.1190/segam2019-3216467.1

Figure 6a shows the effect of varying dither time from the 500 ms in previous examples to 1000 ms on the deblending. Results are very similar when compared to the 500 ms results shown in Figure 5a. The amplitude difference between them is plotted in Figure 6b, and the difference is mostly due to variations in the random noise component. Figure 7a shows the deblending results when the source vessel-to-vessel separation is increased to 10 km, from the 2 km used in the preceding tests, while other parameters are kept constant. The results are quite comparable to the 2 km case shown before in Figure 5a. The deblended gather amplitude difference due to difference in source vessel separation is expressed in Figure 7b, and it does not show any discernable preference for one or the other. Finally, Figure 8 compares the frequency spectrum of the deblended gathers to the target. The 500 ms dithered SS and FF acquisitions with background random noise are used for this comparison. Figure 8a shows that in the low frequency range critical for FWI, less than 2 dB drop in amplitude from the target is observed. The amplitude range of SS and FF acquisitions are identical. The phase response plotted in Figure 8b show that both SS and FF deblended data have very similar response to the target.

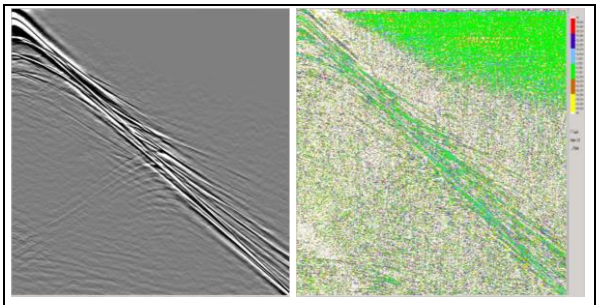

(a) (b)

Figure 7: SS data with 10 km source vessel spacing (a) deblending, and (b) difference from deblending with 2 km source vessel spacing, as percentage of target (green is less than 15% difference).

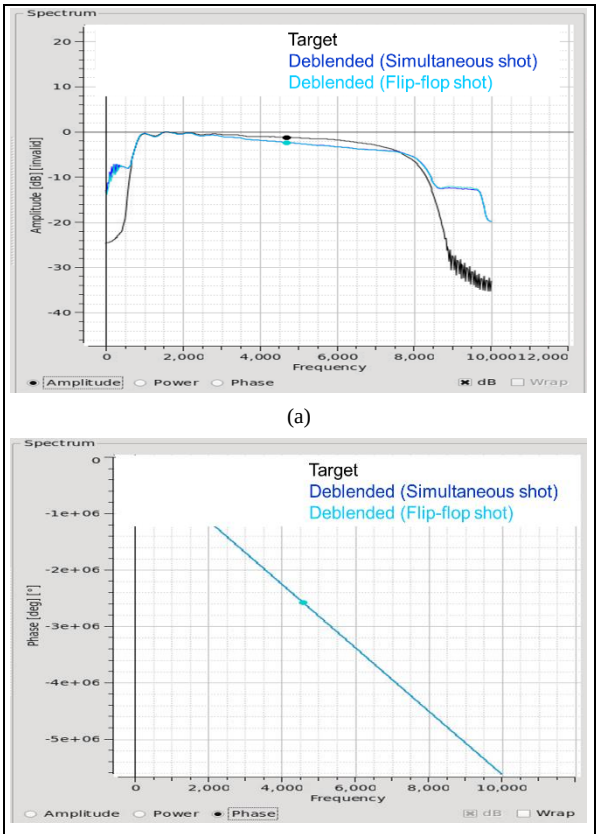

(a)

(b)

Figure 8: Frequency spectrum comparison of target, SS deblended and FF deblended data for (a) amplitude and (b) phase response. For the low frequency zone critical to FWI, less than 2 dB amplitude degradation is observed due to deblending. Amplitude and phase response of SS and FF deblending are similar.

Conclusions

The feasibility of blended acquisition of a very large offset sparse node survey with six concurrent sources is evaluated, with focus on recovering the low frequency diving waves for refraction FWI. A varied range of acquisition parameter are tested, including dither time, source vessel separation, shot firing sequence, and the effect of background random noise. Simultaneous shot and flip-flop shot sequence are extensively compared and shown to perform equally well. It is noted that the inversion based deblending scheme is capable of successfully recovering the diving waves for both schemes of acquisition over the wide range of uncertainties. Strong random noise is shown to cause the most leakage and is particularly detrimental to deblending. Even then all the refractions are discernable, with most events having only 10 to 15% amplitude leakage after deblending. Overall, there is less than 2 dB amplitude loss in the low frequency range due to the blended acquisition. Most importantly, we show that the shot firing scheme has no effect on deblending efficiency for node surveys. Both the SS and FF scheme show similar results, with the difference attributable to random noise.

Acknowledgement

The authors thank Shell for sharing the synthetic receiver gather, and permission to show the data presented. They also thank Connie VanSchuyver for reviewing the manuscript and TGS for permission to publish this work.

10.1190/segam2019-3216467.1

REFERENCES

Abma, R. L., T. Manning, M. Tanis, J. Yu, and M. Foster, 2010, High-quality separation of simultaneous sources by sparse inversion: 72nd Annual International Conference and Exhibition, EAGE, Extended Abstracts, B003, https://doi.org/10.3997/2214-4609.201400611.

Liu, Z., B. Wang, J. Specht, J. Sposato, and Y. Zhai, 2014, Enhanced adaptive subtraction method for simultaneous source separation: 84th Annual International Meeting, SEG, Expanded Abstracts, 115–119, https://doi.org/10.1190/segam2014-1510.1.

Mao, J., J. Sheng, M. Hart, and T. Kim, 2016, High-resolution model building with multistage full-waveform inversion for narrow-azimuth acquisition data: The Leading Edge, **35**, 12031–1036, https://doi.org/10.1190/tle35121031.1.

Masoomzadeh, H., S. Baldock, and Z. Liu, 2018, Deblending continuous records by sparse inversion of energetic and coherent surfaces: 88th Annual International Meeting, SEG, Expanded Abstracts, 4065–4069, https://doi.org/10.1190/segam2018-2995944.1.

Shen, X., I. Ahmed, A. Brenders, J. Dellinger, J. Etgen, and S. Michell, 2018, Full-waveform inversion: The next leap forward in subsalt imaging: The Leading Edge, **37**, 67b1–67b6, https://doi.org/10.1190/tle37010067b1.1.

Tiwari, D., J. Mao, and J. Sheng, 2019, Suprasalt model building using full-waveform inversion: The Leading Edge, **38**, 214–219, https://doi.org/10.1190/tle38030214.1.